한국해양공학회지 제15권 제1호, pp 12~18, 2001 (ISSN 1225-0767)

A Time-Domain Approach for the Second-Order Diffraction Problem Around Circular Cylinders in Random Waves

YONGHWAN KIM
ABS, Research Department, Houston TX

KEY WORDS: Second-order surface flow, Random waves, Rankine panel method, Quadratic transfer function

ABSTRACT: *This study concentrates on the second-order diffraction problem around circular cylinders in multi-frequency waves. The method of solution is a time-domain Rankine panel method which adopts a higher-order approximation for the velocity potential and wave elevation. In the present study, the multiple second-order quadratic transfer functions are extracted from the second-order time signal generated in random waves, and the comparison with other bench-mark test results shows a good agreement. This approach is directly applicable to prediction of nonlinear forces on offshore structures in random ocean.*

1. INTRODUCTION

Oil and gas exploration and extraction have been moving into deeper and deeper waters, and the offshore structures are being designed for operation at stationary positions. Such design includes tension-leg platforms, large spar buoys, and FPSOs. The second-order component plays the key role in the slow-drift motion and springing phenomena. Wave run-up on the body surface is also an important issue related to the freeboard of platform.

In the second-order phenomena, there are two distinct categories; difference-frequency and sum-frequency effects. The difference-frequency effects dictate the slow drift response of an offshore structure restrained by weak restoring mechanisms. Its natural period is of the order of the minutes. On the other hand, the sum-frequency effects are responsible for the excitation of a high-frequency response on the structure and its subsystem in flexural modes with the resonance period being the of the order of a few seconds.

Many studies on the second-order surface flow near offshore structures can be found, and most works of these studies were based on the frequency-domain approach, like Kim (1988). However, the time-domain approach does not hare a matured status yet. Moreover, most of the work was for monochromatic and bichromatic waves. The direct simulation of the second-order wave-body interaction flow in real ocean spectra remains as a challenging topics.

The present study concentrates on multi-frequency waves, aiming the prediction of the multiple linear and quadratic transfer functions on a single run, and finally, the application of a realistic ocean spectrum. The method of solution is a Rankine panel method, which has been developed at MIT. This method adopts the B-spline basis function for approximation of physical quantities, while the body geometry is discretized into flat panels. In addition, a modified Euler scheme is applied for time stepping. Kim, Kring and Sclavounos (1997) have applied this numerical scheme successfully to monochromatic waves. The multi-frequency problem is more complicated than the monochromatic wave in many aspects, and particularly much more computational effort is required.

This paper starts with a brief description of the boundary value problem and the numerical method for the second-order diffraction flow. The convergence of the present numerical method is mentioned for an arbitrary order of basis function, and the consistency and stability are proved. The computational models are circular cylinders, being bottom-mounted or truncated. An integral method of the Fourier transform is used to extract sum- and difference-frequency transfer functions for bichromatic and multi-frequency waves. The computational results are compared with other benchmark test, and a good agreement is observed.

2. FORMULATION

Lets define a Cartesian coordinate at the body center on still water, pointing upward for a positive z coordinate. Assuming the inviscid fluid flows with irrotationality, the linear and second-order velocity potentials and wave elevations can be perturbed from the total velocity potential such that

$$\begin{pmatrix} \Psi \\ \eta \end{pmatrix}(\vec{x}, t) = \begin{pmatrix} \phi_1 \\ \eta_1 \end{pmatrix}(\vec{x}, t) + \begin{pmatrix} \phi_2 \\ \eta_2 \end{pmatrix}(\vec{x}, t) + \ldots \quad (1)$$

The boundary value problems of the linear and second-order diffraction problems are well known. The linear and second-order velocity potential of random or multi-component incident wave can be written as follows:

$$\Phi_{1,I} = \mathrm{Re}\{\sum_j \phi_{1,I}(x,y,z)e^{i\omega_j t}\} \tag{2}$$

$$\Phi_{2,I} = \mathrm{Re}\{\sum_l \sum_m [\phi^+_{2,I}(x,y,z)e^{i(\omega_l+\omega_m)t} + \phi^-_{2,I}(x,y,z)e^{i(\omega_l-\omega_m)t}]\} \tag{3}$$

where the subscript 1,2 means the order of problem. In the second-order wave, there are sum- and difference-frequency components. The free-surface boundary conditions on z=0 becomes

$$\frac{\partial \varphi_k}{\partial t} + g\eta_k = \delta_{2,k}(-\frac{1}{2}\nabla\varphi_1 \cdot \nabla\varphi_1 - \eta_1 \frac{\partial^2 \varphi_1}{\partial z \partial t}) \tag{4}$$

$$\frac{\partial \eta_k}{\partial t} - \frac{\partial \varphi_k}{\partial z} = \delta_{2,k}(-\nabla\varphi_1 \cdot \nabla\eta_1 + \eta_1 \frac{\partial^2 \varphi_1}{\partial z^2}) \tag{5}$$

where $\delta_{2,k}$ means the delta function, which becomes unit in the second-order problem, i.e. k=2. Therefore, the second-order problem requires the linear solution and its past history.

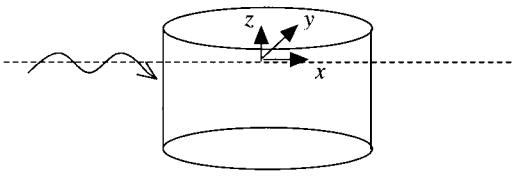

Fig. 1 Coordinate system

A no-flux condition must imposed on the body surface and other rigid boundary.

$$\frac{\partial \Phi_k}{\partial n} = 0 \tag{6}$$

Moreover, the uniqueness of solution is guaranteed when the radiation condition is implemented properly in far field.

The hydrodynamic forces can be obtained by the pressure integration of the linear and second-order pressure,

$$\vec{F_1} = -\rho \int\int_{S_B} \frac{\partial \varphi_1}{\partial t} \vec{n}\, ds \tag{7}$$

$$\vec{F_2} = -\rho \int\int_{S_B} (\frac{\partial \varphi_2}{\partial t} + \frac{1}{2}\nabla\psi_1 \cdot \nabla\varphi_1)\vec{n}\, ds + \frac{1}{2}\rho g \oint_{wl} \zeta_1^2 \vec{n}\, dl \tag{8}$$

3. NUMERICAL METHOD

3.1 Rankine Panel Method

A Rankine panel method has been used to solve the boundary value problem described above. There are many variations of the Rankine panel method, but the present study adopts the numerical scheme developed by Sclavounos (1988) for steady forward-speed problem and Nakos (1993) for the unsteady ship motion, particularly Kim *et al* (1997) for the second-order problem. This numerical method adopts flat panel, but the physical quantities are approximated using a B-spline basis function,

$$\phi(\vec{x}_i, t) \approx \sum_j \phi_j(t) B_{ij}(\vec{x}_i) = \sum_j \phi_j(t) b^{(p)}(\xi; \vec{x}_i) b^{(q)}(\zeta, \vec{x}_i) \tag{9}$$

where (p) and (q) are the degrees of the B-spline function on two coordinates along panel surface.

Time integration scheme is a modified Euler method, and the free-surface boundary conditions are written as follows:

$$\frac{\eta_k^{n+1} - \eta_k^n}{\Delta t} - \Phi^n_{z,k} = \delta_{2,k} P_{kin}(\Phi_1^{n+1}, \eta_1^{n+1}) \tag{10}$$

$$\frac{\Phi_k^{n+1} - \Phi_k^n}{\Delta t} + g\eta_k^{n+1} = \delta_{2,k} P_{dyn}(\Phi_1^{n+1}, \eta_1^{n+1}) \tag{11}$$

where P_{kin} and P_{dyn} mean the forcing terms of equation (4) and (5). In addition, and Δt is time segment and the superscript indicates the time step.

The velocity potential on solid boundary and normal flux on free surface can be obtained from Greens identity such that

$$(\varphi_k)_j^{n+1} B_{ij} + (\varphi_k)_j^{n+1} \int\int_S B_{ij}(\vec{\xi}) \frac{\partial}{\partial n} G(\vec{x}; \vec{\xi}) d\xi$$

$$= (\frac{\partial \varphi_k}{\partial n})_j^{n+1} \int\int_S B_{ij}(\vec{\xi}) G(\vec{x}; \vec{\xi}) d\xi = 0 \tag{12}$$

The radiation condition is imposed using the artificial damping zone. In this zone, the kinematic free-surface boundary condition takes the following form:

$$\frac{\partial \eta_k}{\partial t} - \frac{\partial \varphi_k}{\partial z} + \mu_1 \eta_k + \mu_2 \varphi_k = \delta_{2,k} P_{kin} \tag{13}$$

The first additional term plays the key roll to damp the movement of free surface, while the second extra term prevents the change of the linear dispersion characteristics in this zone. The optimum combination of two terms is when $\mu_2 = -\mu_1^2/4g$ (Kim *et al* (1997)).

3.2 Stability Issue

The stability analysis for the numberical scheme with bi-quadratic basis function was Introduced by Kim *et al* (1997) for the second-order diffraction problem, applying the same idea with Scalvounos and Nakos (1988), and Nakos(1993). This analysis applies a triple discrete Fourier transformation for time segment Δt and constant panel spaces, Δx and Δy.

$$\tilde{f}(u,v,\omega) = \Delta x \Delta y \Delta t \sum_l \sum_m \sum_n f_{l,m}^{(n)} e^{i(ul\Delta x + vm\Delta y - \omega n \Delta t)} \tag{14}$$

Then the numerical dispersion relation in the discrete domain

takes the following form:

$$W(u,v,\omega)=e^{2i\omega\Delta t}-(2-g\Delta t^2 S)e^{i\omega\Delta t}+1=0 \tag{15}$$

when (u,v) is the characteristic wave number of (x,y) coordinates and ω is the wave frequency. $S(u, v)$ is the function of the wave number, and it is related with the Fourier transformation of basis function and Rankine source. For the arbitrary orders of basis function defined in equation (9), the general form of $S(u, v)$ for arbitrary orders of (p) and (q) is written as follows:

$$\begin{aligned}S(u,v)=&\frac{1}{\sqrt{u^2+v^2}}+\frac{(-1)^{p+1}\Delta s(v\Delta s)^{q+1}}{(v\Delta s+2\pi)^{q+1}\sqrt{(u\Delta s)^2+(v\Delta s+2\pi)^2}}\\&+\frac{(-1)^{q+1}\Delta s(u\Delta s)^{p+1}}{(u\Delta s+2\pi)^{p+1}\sqrt{(u\Delta s+2\pi)^2+(v\Delta s)^2}}\\&+\frac{(-1)^{p+q+2}\Delta s(u\Delta s)^{p+1}(v\Delta s)^{q+1}}{(u\Delta s+2\pi)^{p+1}(v\Delta s+2\pi)^{q+1}\sqrt{(u\Delta s+2\pi)^2+(v\Delta s+2\pi)^2}}\\&+O(\Delta s^{p+q+3})\end{aligned} \tag{16}$$

It is easy to find that it approaches the inverse of continuous wave number when $\Delta S=O(\Delta x, \Delta y)\to 0$, so that equation (15) recovers the continuous dispersion relation as $\Delta t\to 0$.

When the magnitude of $e^{i\omega\Delta t}$ is greater than unit, the numerical solution becomes unstable. Figure 2 shows the contour plot of $S/4\beta^2$ where β is $\sqrt{\Delta x/g\Delta t^2}$, which plays a key role for stability. The stable computation is expected when $S/4\beta^2$ is less than 1.0. The basis functions are bi-quadratic in figure (a) and bi-cubic in figure (b). Figure (a) and figure (b) show almost identical stability zones, so we can conclude that, in the viewpoint of stability, the order of basis function may not be higher than bi-quadratic. Therefore, the present computation adopts the bi-quadratic basis function.

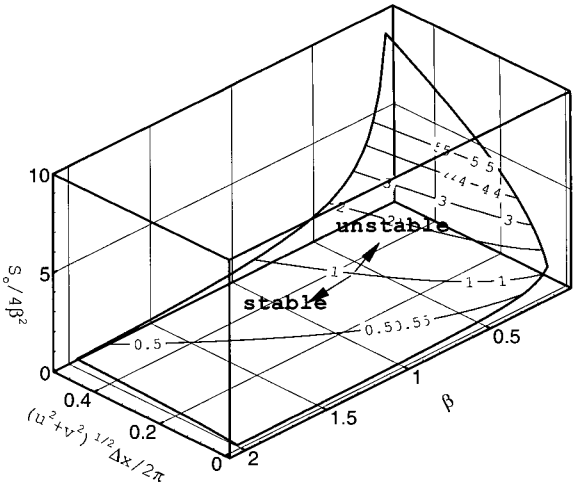

(a) Bi-quadratic basis function

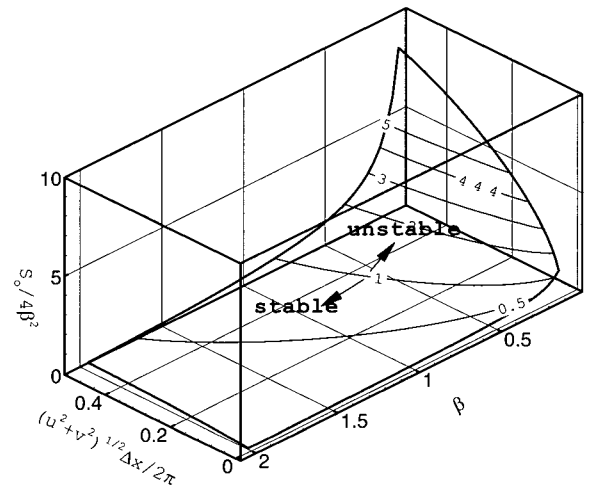

(b) Bi-cubic basis function

Fig. 2 Contour plots of $S/4\beta^2$ and stability zone; $\alpha=1.0$, $p=q=2(a), 3(b)$

3.3 Fourier Transform

The FFT scheme is popular in the Fourier transform of time signal. However, FFT has some restrictions for the selection of frequency. In the present study, the Fourier transform suggested by Kim *et al* (1997) is applied. This method has an advantage that the component can be extracted for any arbitrary frequency as long as the signal is longer than the corresponding period.

When a function is written as the sum of a constant and the series of exponential function,

$$f(t)=C_0+\sum_{k=1}^{N}C_k e^{i\omega_n t} \tag{17}$$

its integral with respect to time should be also satisfied as follows:

$$\int_{T_1}^{T_2} f(t)\,e^{i\omega_m t}\,dt=C_0\int_{T_1}^{T_2} e^{i\omega_n t}+\sum_{k=0}^{N}C_k\int_{T_1}^{T_2} e^{i(\omega_n+\omega_m)t}\,dt \tag{18}$$

Here the weight function is an exponential function with frequency, ω_m. The integrals in right-hand side are trivial and the analytic solution is well known, while the left integral must be obtained using numerical integration. When we apply (N+1) frequencies, which are equal to the basis frequencies of $f(t)$, a matrix equation for unknown C_k can be assembled. In the second-order problem, both sum- and difference-frequencies should be applied in equation (18).

4. COMPUTATIONAL RESULT

The computation was carried out for single cylinders, being bottom-mounted and truncated. Polar grid system with proper stretching near the body was applied. Figure 3 shows an example of solution grids for a bottom-mounted cylinder. In the simulation of multi-component wave, the solution grid must be fine enough to resolve the shortest wave and the computational domain should be large enough to cover the longest wave. Usually, in the second-order problem, the former comes from the sum-frequency components and the latter from the difference-frequency.

Figure 4 compares the computed surge QTF (quadratic transfer function) with Kim's (1988) for a bottom-mounted cylinder shown in figure 3. In this case, the incident wave is bichromatic, and one frequency is fixed as $k_1a=1.2$. The agreement is very favorable.

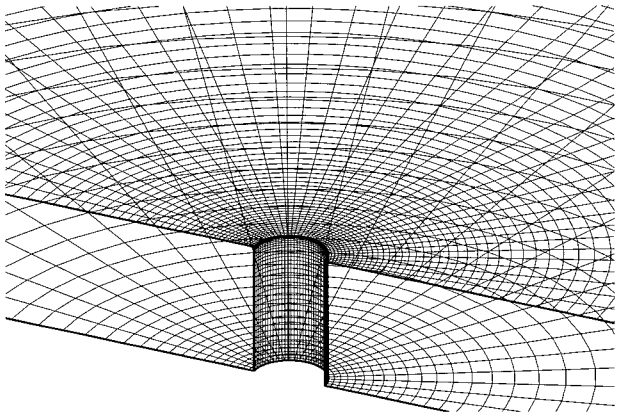

Fig. 3 Solution grids for a bottom-mounted cylinder, depth(h)/radius(a)=4.0

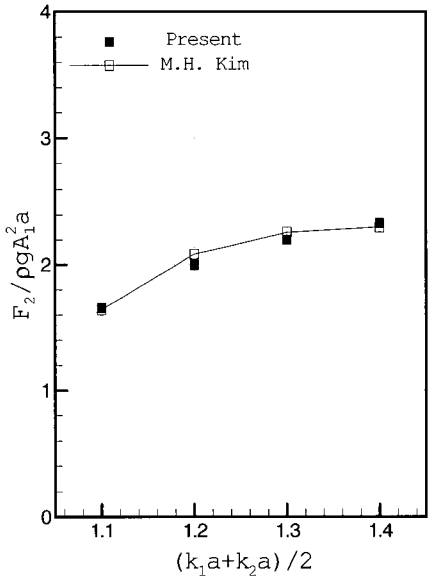

Fig. 4 Surge QTF obtained from the bichromatic force signal; the same cylinder with figure 4, $k_1a=1.2$ (fixed)

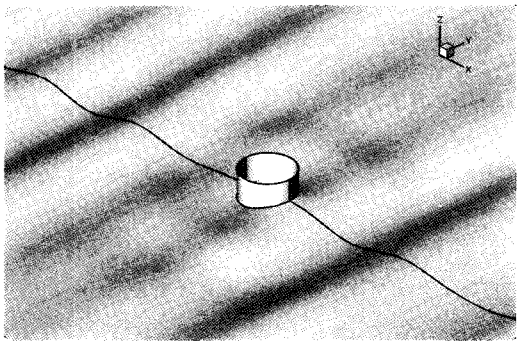

(a) Linear wave

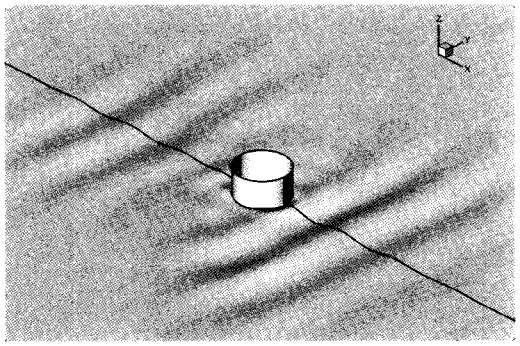

(b) Second-order wave

Fig. 5 Instantaneous linear and corresponding second-order wave profile around a cylinder; h/a=4.0, ka=1.0, 1.2, 1.4, 1.6

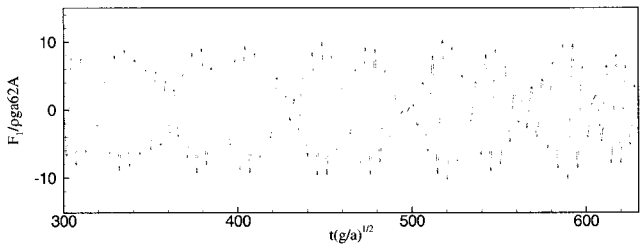

(a) Linear signal

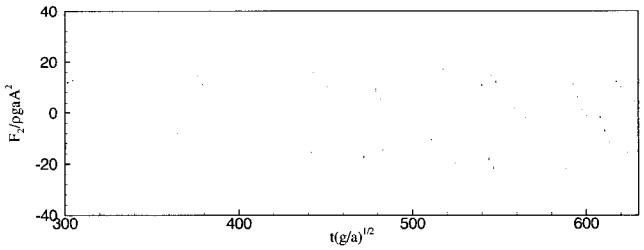

(b) Second-order signal

Fig. 6 The linear and second-order surge force signals on a bottom-mounted cylinder, the same case with figure 5

Figure 5 shows the snapshot of the instantaneous linear and corresponding second-order wave profile around a bottom-mounted cylinder, and the linear incident waves have four different frequencies. ka=1.0,1.2,1.4,1.6. The time histories of the corresponding linear and second-order surge forces are shown in figure 6. Four components are mixed in the linear signal, so that the 16 (4X4) sum-frequency and 16 (4X4) difference-frequency components are mixed in the second-order signal.

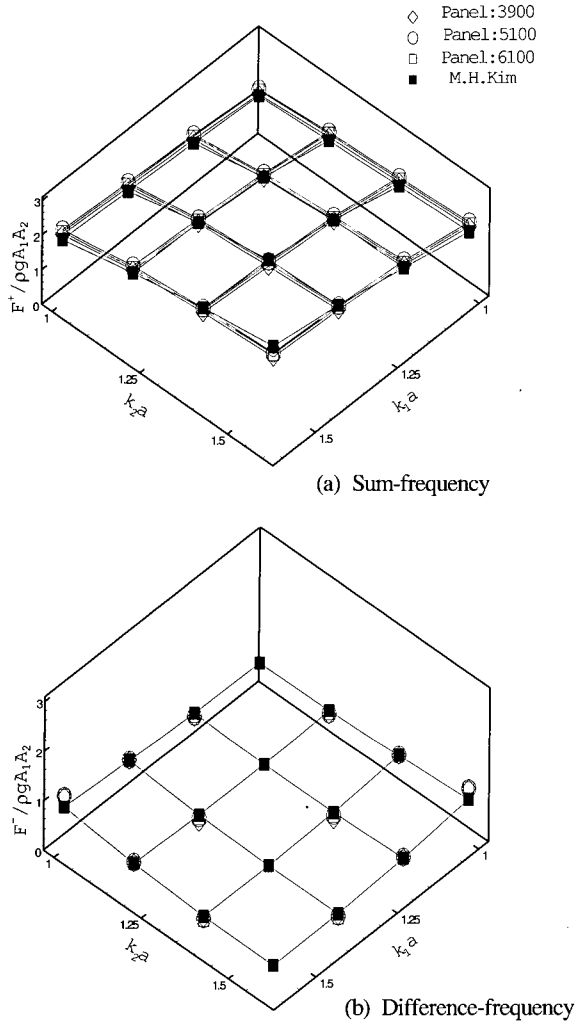

Fig. 7 Grid dependency of Surge QTF matrices, computational domain; 80a, ka=1.0, 1.2, 1.4, 1.6

The linear and quadratic transfer functions can be extracted from these signals using the Fourier transform described above, and the results are shown in figure 7, 8, and 9. One of advantages in the present method is that the four by four QTF matrices of sum- and difference-frequency can be obtained at once from a single signal. In the frequency-domain approach, all combinations of bichromatic waves should be considered to get these matrices.

Figure 7 shows the grid dependency of surge QTF matrices. Since the grid resolution is an important issue in numerical analysis, the observation of grid dependency is essential. Figure 7 shows the comparison of the QTF matrices for three different grid numbers with Kim's result (1988). Both sum- and difference-frequency components shows a good agreement. Moreover, it is obvious that the present numerical scheme is not sensitive on the number of grids as long as the resolution near body is fine enough for the shortest wave.

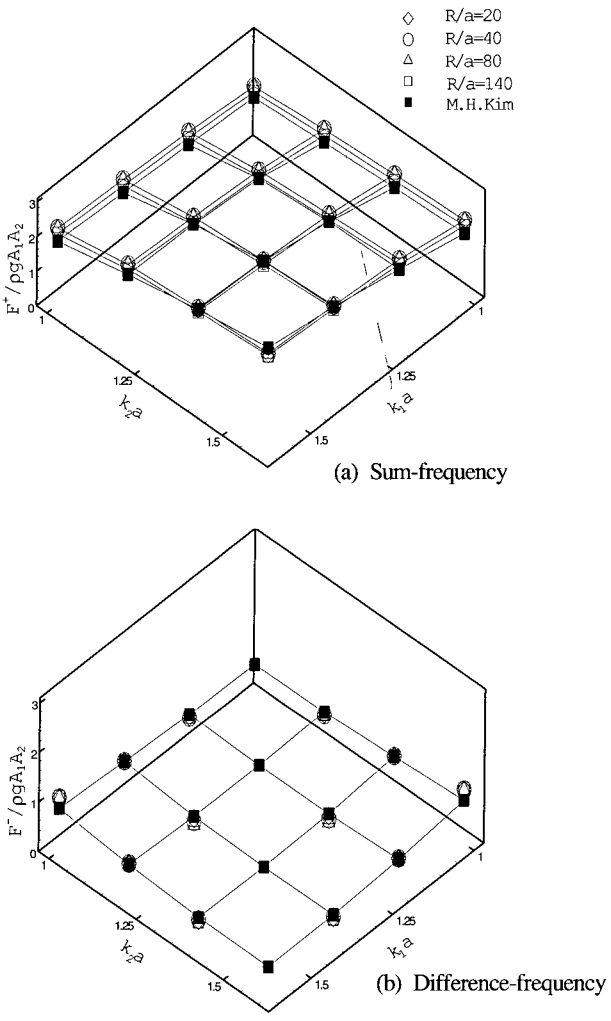

Fig. 8 Domain-size dependency of Surge QTF matrices

Figure 8 shows the dependency on the computational domain. Domain size may be important for the difference-frequency components. The longest wavelength in the present case is 150a, but it is very interesting that the result is quite reasonable even with 20a. As well known, the surface memory effect is important in the second-order problem, so that usually a few times of second-order wavelength should be taken into account in a frequency-domain method. However, the present result shows that,

in a time-domain method, the computational domain may not stretch very far. In the time-domain approach, the distance of wave propagation depends on simulation time, and memory effect can be considered properly as long as the radiation condition is well imposed.

Numerical tests were carried out also for the different time steps, the parameters for artificial damping zone and the time window for Fourier transform, but any significant sensitivity is not found.

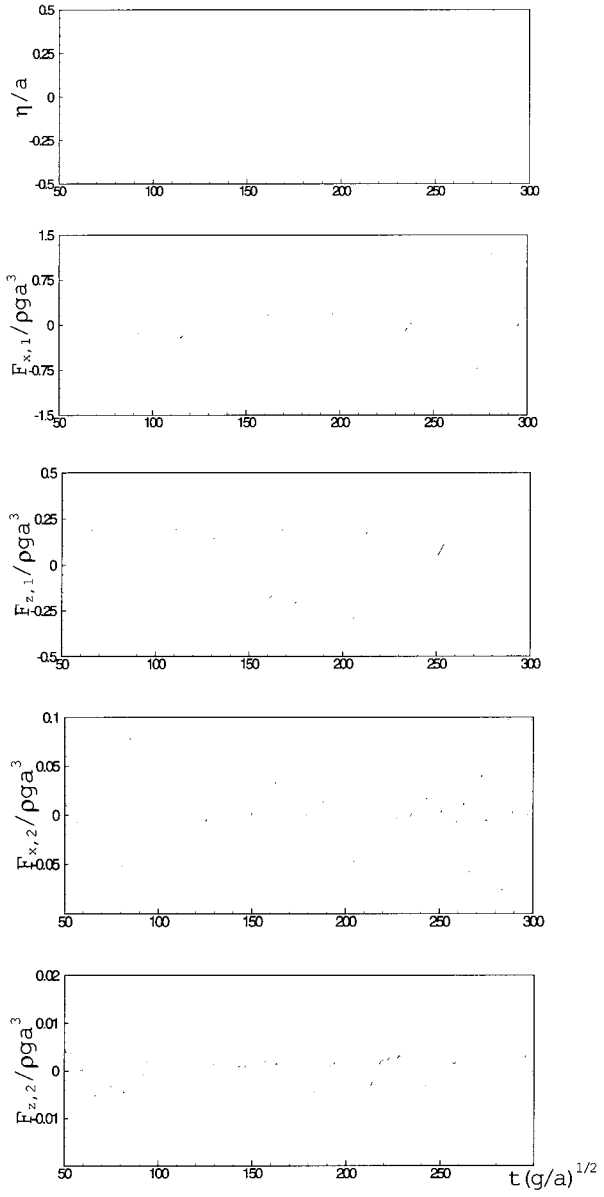

Fig. 9 The wave and corresponding forces on a truncated circular cylinder, draft/radius=4.0, ITTC wave spectrum, sea state 6; from above, input wave at $(x,y)=(0,0)$, the linear surge & heave forces, the second-order surge & heave forces

The present computational method can be easily extended to random ocean spectra. Figure 9 shows the input wave and the corresponding forces on a truncated cylinder. The incident wave has 30 components from ITTC spectrum, sea state 6. The significant wave height is 5.0m and the modal period is 12.4sec. Therefore, the second-order signals have 1800 components, i.e. 900 from sum-frequency and 900 from difference-frequency. The Fourier transform applied in the present method is not valid in the analysis of these signals, and a nonlinear statistical scheme should be applied. Some studies can be found for the analysis of experimental data, and most of them have applied Volterra series. The application of the nonlinear statistic method to the computed time signal brings some issues and difficulties, so that a thorough study is necessary.

5. CONCLUSIONS

The present study focused on the diffraction problem in multi-frequency waves. The linear and second-order boundary value problems have been solve by Rankine panel method, which adopts the bi-quadratic B-spline basis function for the physical parameters. A modified Euler scheme has been applied for the time stepping. From this study, the following conclusions can be made:

- The numerical scheme presented in this study has the consistence and stability, so that the discrete dispersion relation is recovered when the spatial and temporal discretizations become small.
- The computational results don't show any significant dependency on computational parameters as long as the grid resolution near body is fine enough for the shortest wave.
- The quadratic transfer functions showed a good agreement with other benchmark test, and the present numerical scheme can be extended directly to the realistic ocean waves.
- More detailed study is required for the analysis of the second-order signals in random ocean spectra.

REFERENCES

Kim, M. H. (1988). "The complete second-order diffraction and radiation solution for a vertical axisymmetric body", *PhD Dissertation*, Department of Ocean Engineering, MIT, Cambridge, MA.

Kim, Y., Kring, D. C., Sclavounos, P. D. (1997). "Linear and nonlinear interactions surface waves bodies by a three-dimensional Rankine panel methods", *Applied Ocean research*, Vol. 19, pp 235~249.

Kim, Y. (1998). "Computation of higher-order hydrodynamic

forces on ships and offshore structures in waves", *PhD Dissertation*, Department of Ocean Engineering, MIT, Cambridge, MA.

Kim, Y., Sclavounos, P. D. (1999). "Numerical simulation of the linear and second-order surface flows around circular cylinders in random waves", *Proc. of Internation Workshop of Water Waves and Floating Bodies*, pp 80~84.

Nakso, D. E. (1993). "Stability of transient gravity waves on a discrete free surface", *MIT report*, Department of Ocean Engineering, Cambridge, MA

Sclavounos, P. D. & Nakos, D. E. (1988). "Stability analysis of panel methods for free surface flows with forward speed", *Proc. of 17th Naval Shiphydrodynamics*, Hague, the Netherland.

2000년 11월 11일 원고 접수
2001년 1월 28일 수정본 채택